Supplemental Information:

Supplemental Figure Legends:

Supplemental Figure 1: Hierarchy of CD8 T cell response magnitude after rAd vaccination in blood or tissue. Tetramer+ CD8+ T cell responses in **(A)** blood or **(B)** lung at memory (day 70) after vaccination with human-, chimp- or simian-derived rAd vectors. Mice received all rAds at 1 x 10^8 PU; rAd35 was administered at both 1 x 10^9 PU (rAd35hi) and 1 x 10^8 PU (rAd35lo). Bars and errors= mean ± SEM. NS= not significant, *= $p \leq 0.05$ and **= $p \leq 0.01$. Data represent at least two independent experiments (n=3-6; Mann-Whitney test).

Supplemental Figure 2: Gating strategy for defining DC subsets in vivo. Flow cytometry plots illustrating the gating strategy with CD11c+ enriched samples to delineate major DC subsets and evaluate eGFP expression after rAd vaccination.

Supplemental Figure 3: Distribution of Ag to DC subsets after rAd vaccination at varying doses. Pie graphs represent the relative proportion of Ag+ CD11c+ DCs that distribute to each DC subset after vaccination with rAds expressing eGFP. Numbers below each pie graph represents the total number of Ag+ CD11c+ DCs recovered per sample. Numbers in bold with * indicate that fewer than 500 Ag+ CD11c+ DCs were recovered, representing the limit of detection for this assay. Mice received 1 x 10^9, 5 x 10^9 or 5 x 10^8 PU of the rAd vector subcutaneously as indicated

and dLN were harvested at 24 hours after vaccination. Data represent one experiment with 10 dLN pooled from 5 individual mice**.**

Supplemental Figure 4: Role of NK cells subsets in the CD8 T cell response to rAd vaccination. (A) The proportion total leukocytes isolated from the dLN at 24 hours after rAd vaccination contributed by various cell subsets: the total leukocyte composition (**top**); enlarged section to visualise frequencies of rarer populations (**mid-upper**); monocytes **(mid-lower);** B cells **(bottom)**; with significance indicated as compared to the PBS control. **(B)** Validation of depletion of NK cells. **(C)** The frequency of CD8+ T cells expressing IFNγ at 21 days after vaccination using ICS of splenocytes. Bars and errors= mean ± SEM. NS= not significant, *= $p \leq 0.05$ and **= $p \leq 0.01$.Data represent one experiment (n=4-5; Mann-Whitney test).

Supplemental Figure 5: Type I IFN and IP-10 production after rAd vaccination in *STING* gt/gt mice. Amount of IP-10 detected in serum after vaccination of WT or *STING* gt/gt mice with **(A)** 3 x 10^7 PU at 8 hours or **(B)** 1 x 10^8 PU at 6 hours of rAd5, rAd28, rAd35 or chAd63. Amount of **(C)** IFNα or **(D)** IP-10 detected in serum at 6 hours after vaccination of WT or *STING* gt/gt mice with 1 x 10^8 PU of rAd5, rAd35 or chAd63. On scatter graphs, symbols represent individual mice and lines= mean ± SEM. On line graphs, symbols= mean ± SEM. *= $p \leq 0.05$, **= $p \leq 0.05$ for *STING* gt/gt compared to WT. Data represent one experiment (n=4-6; Mann-Whitney test).

Supplemental Figure 6: CD8 T cell responses after rAd28 vaccination in *STING* gt/gt mice. Tetramer+ CD8+ T cell responses after vaccination of WT or *STING* gt/gt mice with 3 x 10^7 PU rAd28. Bars and errors= mean ± SEM. Data represent two independent experiments (n=4-5).

Supplemental Figure 7: CD8 T cell memory and secondary responses after rAd vaccination in *STING* gt/gt mice. (**A)** Frequency of tetramer+ CD8+ T cells in blood at day 30 after vaccination with 3 x 10^7 PU of rAd5 or chAd63 in WT or STING gt/gt mice. **(B)** Bacterial load in spleen after challenge with *L. monocytogenes* expressing Gag at day 35 after vaccination. (**C)** Frequency of tetramer+ CD8+ T cells in blood at day 150 after vaccination. **(D)** Bacterial load in spleen after challenge with *L. monocytogenes* at day 157 after vaccination. (**E)** Frequency of tetramer+ CD8+ T cells in blood directly pre-boost (day 150 post priming with 3 x 10^7 PU of rAd5 or chAd63) and 2 weeks post-boost (day 165) with 100 μg of SIV-Gag AL11 peptide adjuvanted with Poly I:C. Bars and errors= mean ± SEM. NS= not significant, *= $p \leq 0.05$ and **= $p \leq 0.01$. Dotted line= LOD. Data in **(A-D)** represent one experiment and in **(E)** represent two independent experiments (n=3-6; Mann-Whitney test).

Supplemental Tables:

(These are large excel files that are uploaded separately)

Supplemental Table 1: List of all differentially regulated genes that achieve significance at 8, 24 or 72 hours after vaccination with rAd vectors.

Supplemental Table 2: Definition of rAd responsive modules using co-expression analysis.

Supplemental Table 3: Genes that comprise rAd responsive modules and previously defined modules.

Supplemental Table 4: Genes that are consistently up- or down-regulated by all rAds and exhibit diversity in terms of gene expression dynamics.

Supplemental Table 5: Enrichment analysis of genes in Supplemental Table 4.

Supplemental Table 6: Gene- and module-level associations between innate immune responses and Ag expression (restricted to gene co-expression modules).

Supplemental Table 7: Genes with 24 hour fold changes that are significantly associated with Ag expression at 72 hours (unrestricted analysis).

Supplemental Table 8: Module and gene set enrichment analysis of genes in Supplemental Table 7.

Supplemental Methods:

Microarray data analysis:

Step 1 - Microarray dataset

Each microarray comes from an RNA sample obtained from a unique mouse. There were no repeated RNA samples obtained from any mouse. 207 arrays were run overall; 189 from dLN and 18 from PBMCs obtained from mice vaccinated subcutaneously with different rAd vectors. The dLN arrays were run in three batches, denoted A-C, and the PBMC arrays were run in Batch D. **Batch A = 108 arrays**. Batch A consisted of six biological replicates at each of three time points (8, 24 and 72 hours) post-vaccination with PBS, rAd5 (1 x 10^8 PU), rAd28 (1 x 10^8 PU), rAd35 (1 x 10^9 PU), sAd11 (1 x 10^8 PU) and sAd16 (1 x 10^8 PU). **Batch B = 46 arrays**. Batch B consisted of four biological replicates at each of three time points (8, 24 and 72 hours) post-vaccination with chAd3 (1 x 10^8 PU), chAd63 (1 x 10^8 PU) and Poly I:C. Batch B also consisted of two biological replicates at each of three time points (8, 24 and 72 hours) post-vaccination with rAd5 (1 x 10^8 PU) and four biological replicates at each 8 hour time point post-vaccination with PBS (control). **Batch C = 35 arrays**. Batch C consisted of five biological replicates at the 8 hour time point post-vaccination of WT, *IFN$\alpha\beta$R*$^{-/-}$ and *STING* gt/gt mice with PBS and chAd63 (3 x 10^7 PU). Batch C also consisted of five biological replicates from WT mice at the 8 hour time point post-vaccination with rAd5 (3 x 10^7 PU). **Batch D = 18 arrays**. Batch D consisted of the PBMC microarray set, which included six biological

replicates at each 24 hour time point post-vaccination with PBS, rAd5 and rAd28 (1 x 10^8 PU).

Step 2 - Microarray normalisation

Microarrays from all three batches were normalized together using the *normalize.quantiles* function in the Bioconductor package (1). Repeated measurements for a given gene were averaged (on a log2 scale) in the following manner: (i) simple averages were computed for repeated measurements of individual probes; and (ii) weighted averages based on 90% expression quantiles were sequentially computed for repeated measures of systematic IDs and gene symbols.

Step 3 - Selection of genes significantly impacted by vaccination in WT dLN

The initial analysis was based on 142 microarrays from dLN batches A and B (above) measured at each of three time points (8, 24 and 72 hours) post-vaccination with PBS (control, n=6-10), rAd5 (1 x 10^8 PU, n=8), rAd28 (1 x 10^8 PU, n=6), rAd35 (1 x 10^9 PU, n=6), sAd11 (1 x 10^8 PU, n=6), sAd16 (1 x 10^8 PU, n=6), chAd3 (1 x 10^8 PU, n=4) and chAd63 (1 x 10^8 PU, n=4). Starting from 35540 unique genes, 14169 genes exhibiting 90% normalized log2 expression intensity quantiles that exceeded a value of 8 were retained for subsequent analysis. Log2 expression values for each gene were standardised to fold changes with respect to PBS by subtracting the overall average log2 PBS expression value (across all time points) for that gene in the same batch. Genes with log2 expression values that were significantly affected

by vaccination (different between vectors and/or PBS) were then identified using F-tests (ANOVA in R) to compare two different linear expression models:

- *Model1*: l2e ~ V + T + V:T
- *Model2*: l2e ~ T

In these models, "l2e" is the batch standardised log2 expression fold change for the gene compared to PBS, V is the fixed effect for vector (levels: PBS, rAd5, rAd28, rAd35, sAd11, sAd16, chAd3 and chAd63), T is the fixed effect for time (levels: 8hrs, 24hrs and 72hrs) and V:T represents the vector*time interaction.

P-values from the F-test comparing *Model1* and *Model2* were adjusted to false discovery rates (FDR) using the Benjamini-Hochberg algorithm. The FDR threshold for significant impact of vaccination on expression was set at 0.001, which yielded 10902 genes. Of these, only those exhibiting an absolute average log2 fold difference compared to PBS that exceeded 1 for at least one vector for at least one time point were retained for downstream analysis. This final filtering step yielded 3888 genes, which are shown in Figure 4A and Supplemental Table 1. The clustered and scaled heat-map visualisation of the results (Figure 4A) was generated using Cluster 3.0 and Treeview (2).

Step 4 - Canonical pathway enrichment analysis

Canonical pathway enrichment analysis of the 3888 genes significantly impacted by vaccination and gene co-expression modules (defined below) was performed using Ingenuity Pathways Analysis software (Ingenuity Systems Inc., Redwood City, CA).

Step 5 - Defining gene co-expression modules

The algorithm described below for constructing gene co-expression modules was developed with two major objectives in mind: (i) data reduction through the identification of major groups of genes with sufficiently coherent expression patterns to justify analysis at the level of collective average expression; and (ii) identification of these groups in a data-driven manner, without prior specification of the number of modules, number of genes per module or specific expression patterns within the modules.

5.1 - Gene selection: The 3888 genes significantly impacted by vaccination that exhibited differential responses between the rAd vectors were first identified by repeating the F-tests comparing *Model1* and *Model2*, but this time the analysis was performed without including the PBS samples. Again, F-test p-values were adjusted to FDRs using the Benjamini-Hochberg algorithm and the significance threshold was set at FDR ≤ 0.001, yielding 3771 genes. This set of genes was further refined by only retaining those that exhibited appreciable variation between vectors (standard deviation of log2 expression fold changes across all vectors ≥ 0.5 for at least one time point), yielding a final set of 1459 genes.

5.2 - Defining co-expression modules: Groups of genes expressing well-defined and strongly concordant patterns of expression (co-expression modules) were constructed in the following manner from the 1459 genes selected above:

a) Average log2 expression fold changes (compared to PBS) were computed for every gene for each vaccine vector for each time point, and then scaled by the maximum absolute average log2 expression observed for each gene. This

matrix of scaled average expression values was then clustered in a hierarchical manner using Cluster 3.0 (Similarity metric = uncentered correlation, Clustering method = centroid linkage) (2).

b) "Seed" modules were then constructed by first evaluating the Pearson correlations between adjacent genes in the clustered expression matrix, and then retaining stretches of genes that exhibited strong correlation. Requiring stretches to include 10 or more genes with Pearson correlations ≥ 0.7 identified 20 candidate seed modules consisting of 12-209 genes (median = 38 genes).

c) In order to account for the randomness inherent to the initial clustering, the seed modules were refined to include other genes that were as strongly correlated to the average seed module expression as the constituent genes within the seed modules, and genes with low correlations to the average seed module expression were excluded. Genes with Pearson correlations to seed module average expression that were ≥ the 25% quantile of Pearson correlations between seed module genes and the seed module average expression were added to the seed modules, and seed module genes with correlations to module average expression less than this threshold were excluded from the module. The Pearson correlation coefficient thresholds for adding/excluding genes from the seed modules ranged from 0.85-0.95 (median = 0.90). Genes that would be assigned to more than one module by this process were assigned to the modules for which these genes had the

strongest Pearson correlation. This process resulted in 20 refined modules consisting of 11-151 genes (median = 42 genes).

d) The average expression profiles of the 20 refined modules were next compared to each other to evaluate whether some of the modules were redundant in terms of expression pattern. The two modules with the largest Pearson correlation between their average expression values were combined, and module average expression values were recomputed. This processed was repeated for 7 iterations until the maximal inter-module correlation was less than 0.9. This resulted in 14 non-redundant modules, consisting of 11-243 genes (median = 35.5 genes).

e) Finally, step (c) was repeated to expand and render unique (in terms of gene composition) the modules. This generated the final set of 14 gene co-expression modules, consisting of 8-181 genes (median = 30.5 genes). These modules are shown in Figure 6 and Supplemental Tables 2 and 3.

5.3 - Annotation of co-expression modules: GeneMANIA (3) was used to identify cellular functional processes that were over-represented within the gene co-expression modules. Significant (FDR < 0.05) associations were identified for 5 modules (C1, C2, C3, C10, and C11) and a marginally significant (FDR = 7.34E-2) association was observed for module C12. These associations are summarized below.

Co-expression module = C1, annotation = angiogenesis, GeneMANIA enriched function = vascular endothelial growth factor receptor signaling pathway (FDR = 5.6E-11, coverage = 8/36), representative genes = FLT1 and VEGFA.

Co-expression module = C2, annotation = IFN signaling, GeneMANIA enriched function = cellular response to type I IFN / type I IFN signaling pathway (FDR = 1.36E-28, coverage = 22/71), representative genes = Eif2ak2/PKR, Irf7 and Mx1.

Co-expression module = C3, annotation = IFNs, GeneMANIA enriched function = regulation of defense response (FDR = 1.0E-6, coverage = 15/295), representative genes = 7 Ifna species (1, 2, 5, 7, 13, 14, -b), Ifnb1 and Ifng.

Co-expression module = C10, annotation = extracellular matrix ("ECM"), GeneMANIA enriched function = extracellular matrix (FDR = 7.3E-3, coverage = 7/184), representative genes = Itgb5 and Timp2.

Co-expression module = C11, annotation = extracellular matrix ("ECM"), GeneMANIA enriched function = extracellular matrix (FDR = 7.8E-3, coverage = 8/184), representative gene = TAM receptor ligand Gas6.

Co-expression module = C12, annotation = lymphocyte activation ("Lo Act"), GeneMANIA enriched function = lymphocyte activation (FDR = 7.34E-2, coverage = 10/23), representative genes = Cd55, Cd7 and Ltk.

Step 6 - Module-level analysis of gene expression

A modular analysis framework (4) was employed to deconvolute the complex and dynamic dLN transcriptional responses to vaccination.

6.1 - Module definitions: Three sets of modules were used in the analysis: (i) the 14 co-expression modules that were constructed from our dataset using the approaches described above; (ii) the whole blood modules defined by Chaussabel and colleagues (5); and (iii) the immune cell lineage and cell differentiation status-

specific modules defined by the Immunological Genome Project (6). Even though they were developed from human whole blood transcriptome datasets (5), module set #2 was employed because we previously found these modules to be very informative for the interpretation of peripheral transcriptome responses induced by an rAd vaccine in humans (7) and wanted to determine whether blood-based modules could be applied to data derived from LNs. Only modules with assigned functional annotations were employed. Modules that were given the same functional annotation were merged. In this manner, modules M1.2, M3.4, and M5.12 (associated with "Interferon") became a single "Interferon" module, and modules M4.3, M4.5, and M5.9 (associated with "Protein Synthesis") became a single "Protein Synthesis" module. Previously, we employed canonical pathway enrichment analysis to confirm the functional annotations assigned to these modules (7). We used Homologene (8) to map from the human identifiers (through which the modules were defined) to the mouse identifiers employed in the Agilent microarray platform. Module set #3, having been developed through the analysis of sorted immune cell transcriptome compendia (6), was included in the current analysis because it can facilitate deconvolution of the mixed cell population lymph node transcriptomes. For simplicity, we restricted our analysis to the "coarse" modules in this study that were assigned well defined titles that were clearly associated with cellular lineages and/or up-/down-regulation upon differentiation. As for Module set #2, modules that were associated with lineages or processes in common were merged. In this manner, coarse Immgen modules 24, 29-32, and 74 (associated with "Myeloid Lineage") became a single "Myeloid" module, and coarse Immgen modules

11-15 (associated with “Cell Cycle”) became a single “Cell Cycle” module. Altogether, our module-based analysis involved 48 partially overlapping modules that comprised 5337 unique genes. Gene:Module assignments are provided in Supplemental Table 3.

6.2 - Estimating module-level expression: For module-based analysis, module-level expression was estimated in any condition or replicate by taking the average of the normalized log2 expression of all of the genes in that module.

6.3 - Selection of modules significantly impacted by vaccination: Modules (from Sets #2 and #3) that were significantly impacted by vaccination and/or exhibited vaccine responses that differed significantly between vaccines were identified using the approaches for identifying individual genes with the same behavior (steps 3 and 5.1, above), with the exception that the absolute average log2 fold change threshold was set to 0.5 (instead of 1 - step 3), and the standard deviation threshold was set to 0 (instead of 0.5 - step 5.1). Nine modules (from Sets #2 and #3) met these thresholds and are plotted in Figure 6, along with representative gene co-expression modules.

Step 7 – Evaluation of the dynamical diversity in rAd induced gene expression responses

7.1 - Defining patterns of induction (or repression) for each gene for each vector: The starting point of this analysis was the set of 3888 genes that were significantly differentially expressed in response to rAd vaccination (the result of *Step 3 - Selection of genes significantly impacted by vaccination in WT dLN*). For each

gene for each vector for each time point, a simple non-paired heteroskedastic t-test was performed comparing gene expression after vaccination with rAds to PBS at the same time point. Significant differential expression for a given gene for a given vector at a given time point was defined as $p<0.05$ and Avg log2 FC > 0.5 for up-regulation, and $p<0.05$ and Avg log2 FC < -0.5 for down-regulation. These nominal significance thresholds were applied in this analysis because the starting set of 3888 genes was already the result of extensive statistical filtering. Genes were then selected that exhibited differential expression for all seven vectors for at least one time point (8, 24 or 72 hours), but did not exhibit uniformity across all vectors and all time points. Up-regulation and down-regulation were analyzed separately, and we identified 526 up-regulated and 758 down-regulated genes that met these criteria. The gene sets and associated patterns of differential expression are provided as 21 element "differential expression vectors" in Supplemental Table 4, where "1" indicates significant differential expression for a given gene in response to a given vector at a given time point.

7.2 – Module enrichment analysis of gene groups with similar dynamics

We next tested whether existing gene modules (5, 9) were over-represented within groups of genes exhibiting similar patterns of dynamical behavior (having similar vectors of 1s and 0s in Supplemental Table 4). Mouse symbols were mapped to human symbols for compatibility with the module definitions using Homologene. Partially overlapping gene groups were constructed for each observed differential expression vector ("seed") from all of the genes with differential expression vectors that differed from the seed by 1 or 0 elements, allowing for a mismatch to the seed

permitted grouping of genes that were very similar without requiring the stringency of exact matches. Gene enrichments were evaluated using Fisher's exact test. Enrichment tests for up- and down-regulated genes were carried out separately and were only performed for gene groups that contained at least 2 genes after mapping from mouse to human symbols or for modules that contained at least 5 genes within the reference pool. Enrichment p-values for all modules for all gene groups were FDR adjusted together using the Benjamini-Hochberg algorithm. Multiple testing corrections for each reference and module selection were performed in a sequential manner: First, all gene groups were tested for over-representation of all modules with respect to all of the genes on the microarray. Enrichment p-values for this reference were adjusted and enrichments with $p<0.05$ and FDR < 0.2 were retained. Second, the surviving gene group/module pairings were tested for enrichments with respect to the starting set of 3888 genes for the dynamical analysis. Enrichment p-values for this reference were adjusted and enrichments with $p<0.05$ and FDR < 0.2 were retained. Finally, the surviving gene group/module pairings were tested for enrichments with respect to the overall with respect to the set of 526 up-regulated genes or 758 down-regulated genes from which the gene group was constructed. Enrichment p-values for this reference were adjusted and enrichments with $p<0.05$ and FDR < 0.2 were retained. This sequential filtering scheme ensures that the multiple testing adjustment is only applied to enrichments of interest. For example, we are not interested in whether a particular gene group is enriched for IFN response compared to the ensemble of up-regulated genes if that gene group is not actually enriched for IFN response compared to the genome.

Lastly, only module enrichments that involved an overlap of at least two genes between the module and the gene group were retained. When a particular module was over-represented within multiple gene groups, the enrichment that involved the greatest overlap between the module and the gene group was retained. When a particular gene group was enriched for multiple modules, the enrichment that involved the greatest overlap between the module and the gene group was retained.

This grouping strategy revealed an unexpected high occurrence of KLRA NK receptors (Ly49 family), and we performed a separate enrichment analysis for a custom "killer cell lectin-like receptor" module that was defined as all of the genes with gene titles containing that phrase. There were 37, 17, and 8 genes from this module on the microarrays, within the set of 3888 differentially expressed genes, and within the 526 up-regulated genes from which the gene groups were constructed, respectively. The final gene group enrichments are enumerated in Supplemental Table 5, and include:

Up-regulated genes-

- Subset of IFN-associated genes; induced by all vectors at 8 and 24 hours, but with rAd5 and sAd16, chAd3 and sAd16, or sAd16 alone lacking persistent induction at 72 hours.
- Killer cell lectin receptor-associated genes (Ly49 family); significantly induced at 72 hours by all vectors, but preferentially induced by rAd5 or chAd3 at 24 hours.

- Subset of cell cycle-associated genes; significantly induced at 72 hours by all vectors, but preferentially induced by rAd28 or chAd63 at 24 hours.
- Subset of monocyte-associated genes; induced at 8 hours by all vectors, and at 24 hours by all vectors except rAd5.

Down-regulated genes-

- DC surface signature- and developmental-associated genes; down-regulated by all vectors at 24 hours, and by all vectors except rAd5, sAd11 and sAd16 at 8 hours.
- Platelet-associated genes; down-regulated by all vectors at 24 hours, down-regulated by all vectors except rAd5 and sAd16 at 8 hours, and persistently down-regulated by all vectors except sAd11, sAd16, and chAd3 at 72 hours.
- Subset of cell cycle-associated genes; down-regulated by all vectors at 24 hours, down-regulated by all vectors except rAd28, sAd11, and sAd16 at 8 hours, and persistently down-regulated by rAd35 and chAd63 at 72 hours.
- Subset of monocyte-associated genes; down-regulated by all vectors at 24 hours, down-regulated by all vectors except sAd16 at 8 hours, and persistently down-regulated by rAd35 and chAd63 at 72 hours.

Step 8 - Comparison of rAd vector responses in dLN and PBMCs

8.1 – Normalizing and integrating human microarray data with mouse data:

The human microarray data from Zak et al. (7) was re-normalized using an Entrez gene-based custom CDF provided by BRAINARRAY (10). Human gene symbols were mapped to mouse using Homologene (8) and only those genes with human and

mouse orthologs on both array platforms were retained for this analysis (16126 genes total). Human gene expression fold changes were computed with respect to pre-vaccination for the same subject. This is in contrast to the mouse expression fold-changes (for both dLN and PBMC) that were computed with respect to the average PBS response at the same time point.

8.2 – Defining concordant and discordant gene expression responses to rAds in PBMC and dLN:

In order to compare PBMC and dLN rAd-induced expression responses, we first defined responses that were consistent across rAds in either tissue.

For dLN, we required that the compilation of all FCs across all vectors for a given gene at 24hrs significantly (FDR < 0.05) differed from 0 by Wilcoxon signed rank test, that the gene was significantly differentially expressed (FDR < 0.05 by t-test) for 4/7 vectors, and that the fold changes for all vectors were either positive or negative (irrespective of statistical significance). In this manner, we were identified 2133 and 3781 consistently up-regulated and down-regulated genes in dLN, respectively.

For PBMCs, we required that the compilation of all FCs across all vectors (rAd5, rAd28, MRKAd5) and species (mouse, human) for a given gene at 24hrs significantly (FDR < 0.05) differed from 0 by Wilcoxon signed rank test, that the gene was significantly differentially expressed (Mouse: FDR < 0.05 by unpaired t-test vs PBS, Human: FDR < 0.05 by paired t-test compared to pre-vaccination) in either human

or mouse for at least one vector, and that the fold changes for all vectors for both species were either positive or negative (irrespective of statistical significance). In this manner we were identified 813 and 818 consistently up-regulated and down-regulated genes in PBMC, respectively.

Concordant and discordant responses between the tissues were then identified by examining the intersections between the various lists. Statistical significance of the intersections was assessed by Fisher's exact test.

8.3 – Module enrichment analysis of concordant and discordant gene lists:

The concordant and discordant gene lists were tested for significant over-representation of gene modules (5, 9). Gene enrichments were evaluated using Fisher's exact test using two reference pools: (1) the set of 16126 genes in the analysis, and (2) the combined set of concordantly and discordantly regulated genes (817 genes total). Enrichment tests were only performed for modules that contained at least 10 annotated genes among the 16126 that were evaluated in this analysis. Enrichment p-values for all modules for all gene groups were FDR adjusted together using the Benjamini-Hochberg algorithm. Multiple testing corrections for each reference and module selection were performed in a sequential manner: First, all gene groups were tested for over-representation of all modules with respect to all genes in the analysis. Enrichment p-values for this reference were adjusted and enrichments with FDR<0.01 and were retained. Second, the surviving gene group/module pairings were tested for enrichments with respect to the combined

set of concordantly and discordantly regulated genes. Enrichment p-values for this reference were adjusted and enrichments with FDR < 0.01 were retained. This sequential filtering scheme ensures that the multiple testing adjustment is only applied to enrichments of interest.

Step 9 - Integrating innate immune responses with rAd vector antigenicity

In contrast to clinical studies, where it is possible to link peripheral innate immune responses longitudinally to subsequent adaptive immune responses in the same subject (7, 11), the mice in the present study were not followed longitudinally. Custom analytical approaches were therefore necessary to identify potential associations between innate activation and vector immunogenicity. Two analytical strategies are described below to achieve this. The first, called "model-based analysis", estimates the statistical significance of the associations using linear modeling and estimates "strength" of associations between innate activation and immunogenicity using "all vs. all" Spearman rank correlations. The second, called "stratified bootstrapping analysis", simultaneously assesses the strength and statistical significance of the associations through a bootstrap resampling based Spearman rank correlation analysis.

9.1 – Model-based analysis: We call the vector of immunogenicity measurements (for example, Ag expression levels measured 72 hours post-vaccination) "*Y*". The vector *Y* consists of *Nyi* replicate measurements from each of the 7 rAd vectors, where "*yi*" indicates immunogenicity measurements for a particular vector *i*. For example, if there were 3 vectors (*i*=1) rAd5, (*i*=2) rAd28 and (*i*=3) chAd63, and

there were 4 replicate measurements for rAd5, 6 replicate measurements for rAd28 and 5 replicate measurements for chAd63, then $Ny1 = 4$, $Ny2 = 6$ and $Ny3 = 5$.

Similarly, we call the vector of innate immunity measurements (for example, log2 fold expression of co-expression module C2 compared to average PBS 24 hours after vaccination) "*X*". The vector *X* consists of *Nxi* replicate measurements from each of the 7 rAd vectors, where "*xi*" indicates innate immunity measurements for a particular vector *i*. Note that these replicates are completely independent from the replicates in *Y*, as there was no longitudinal sampling. If there were 3 vectors (*i*=1) rAd5, (*i*=2) rAd28 and (*i*=3) chAd63, and there were 8 replicate measurements for rAd5, 6 replicate measurements for rAd28 and 4 replicate measurements for chAd63, then $Nx1 = 8$, $Nx2 = 6$ and $Nx3 = 4$.

We then compute the "all vs. all" Spearman correlation coefficient between *X* & *Y* by integrating the two vectors in a manner where we assume that every replicate for a given vector in *X* can be paired with every replicate for the same vector in *Y*. For example, combining the hypothetical vectors *X* and *Y* above in this manner would involve construction of 32 pairs for rAd5, 36 pairs for rAd28 and 20 pairs for ChAd3. Combining these gives matched permuted *X* and *Y* vectors, each 88 elements long, from which the Spearman correlation coefficient can be computed. This "all vs. all" approach is advantageous over simply averaging across replicates and computing correlations because it penalizes within-group variability in either *X* or *Y*.

We then used 2-way ANOVA to estimate the statistical significance of any effect from the different vectors that **consistently** impacted innate immune responses (*X*) and immunogenicity (*Y*). Prior to ANOVA, *X* and *Y* are first transformed into scaled variables: *X*0' = *X*/sd(*X*) & *Y*' = *Y*/*sd*(*Y*), where *sd*() indicates standard deviation. *X*0' was additionally transformed using the sign of the "all vs. all" Spearman correlation coefficient (*R*): X' = *sign*(*R*) * *X*0'. These two transformations serve to ensure that any correlation between *X*' and *Y*' is positive, and that the range of variation in *X*' and *Y*' is comparable. We then fit the following two models:

Model6: $M \sim I$ + V

Model7: $M \sim I$+V+*I*:V

In these models, *M* indicates "measurement" and is either *X*' or *Y*', *I* indicates what type of immune response is being measured (*I*=0 if *M*=*X*, *I*=1 if *M*=*Y*'), V is the fixed effect for vector (levels: rAd5, rAd28, rAd35high, sAd11, sAd16, chAd3, chAd63) and *I*:V indicates interaction between I and *V*.

We seek combinations of *X* and *Y* for which the FDR-adjusted ANOVA p-value for the V term (pV) in Model6 is statistically significant. Since Model6 does not include an interaction term, a statistically significant pV indicates that variation in vector impacts *X*' and *Y*' similarly. In other words, the effects on *X*' of changing from one vector to another are correlated with the effects on *Y*' of changing from one vector to another. Therefore, pV provides some statistical measure of a relationship between

X' and *Y*' across the vectors. If *X* and *Y* are anti-correlated, the sign transformation from *X*0' to *X*' renders *X*' and *Y*' positively correlated, and again the model without the interaction term is appropriate. The scaling transformations attempt to minimize any gross differences in magnitude of variation within X and Y, which also renders the model without interaction term appropriate. As a final evaluation of the relationship between *X* and *Y*, we compute the p-value for the interaction term in Model7 (pIV). Since a significant interaction term would indicate that the effect of changing vector depends on whether *X* or *Y* is measured, we seek *X* and *Y* for which the interaction term is not significant. In practice, we simply seek *X* and *Y* for which pV is much smaller than pIV.

In the present study, *Y* = log expression of SIV Gag in dLN measured 72 hours post-vaccination and *X* = module-level or gene-level fold changes in dLN expression compared to PBS at 8, 24 or 72 hours post-vaccination. We used the following thresholds to identify genes and modules that were significantly associated with Ag expression levels: $|R| \geq 0.75$, pV(adjusted) ≤ 1e-5 and pV/pIV ≤ 1e-5. At these thresholds, we found the largest number of associations between Ag expression levels at 72 hours and innate immune responses at the 24 hour time point, which included 7 modules: co-expression modules C2 (IFN signaling) and C3 (IFNs) exhibited negative associations with Ag expression, while C9, C10, and C14 exhibited positive associations with Ag expression. In addition, two IFN response modules from previous studies were negatively associated with Ag expression. Within the co-expression modules, 91, 20, 3, 7 and 15 genes were significantly

associated with Ag expression for C2, C3, C9, C10 and C14, respectively. These results are compiled in Supplemental Table 5.

9.2 - Stratified bootstrapping analysis: Although the model-based analysis described above provides a rigorous method to assess the association between gene and Ag expression datasets, adjustments for multiple testing are difficult because the approach involves multiple terms (pV, pIV, and R). This alternative approach employs bootstrap resampling to estimate p-values for the association that can be adjusted using conventional methods, permitting large-scale tests of association (for example, between Ag expression and all genes on the microarray) where multiple testing corrections are critical. The underlying assumption in the approach is that each biological replicate measurement of Ag expression could theoretically have been obtained from each mouse in which dLN gene expression was measured.

This approach begins with the "all vs. all" matrix that was employed in 9.1. Stratified bootstrap resampled datasets are constructed from the all vs. all matrix in the following manner: First, the number of biological replicate measurements for gene expression and Ag expression for a given vector are determined, and the average of these two values is computed and rounded down to the nearest integer. For each vector (v) this number is Nv. Next, Nv "rows" from the "all vs. all" matrix corresponding to each vector are randomly sampled with replacement. The resampled rows for each vector are compiled into the stratified bootstrap resampled dataset. Next, straightforward Spearman rank correlation analysis is performed on the bootstrap resampled dataset, producing the p-value and

correlation coefficient. Finally, this bootstrap is repeated for a total of 300 times, generating a distribution of correlation coefficients and p-values for each gene:Ag association. The median p-value from all bootstrap iterations is taken as the summary statistic for the significance of the association. This p-value is readily adjusted for multiple comparisons using standard methods. Confidence intervals on the correlation coefficient are readily estimated from the population of correlation coefficients from the permutations. For visualization of the associations, it is possible to generate an ensemble of nonlinear spline fits linking Ag to gene expression using the collection of bootstrap resampled datasets. In Figures 9B and 9C, 99% confidence intervals utilised the smooth.spline() function in R with 3 degrees of freedom.

Step 10 - Comparing responses to Poly I:C and rAd vaccination

Two analyses were performed that compared the innate transcriptional responses triggered in dLN by the rAd vectors with the responses triggered by Poly I:C.

10.1 - Candidate analysis: In the candidate-based analysis of rAd and Poly I:C-induced responses in dLN, the 23 modules significantly regulated by all vectors in dLN (co-expression modules C1-14 and the nine significantly regulated modules from Module Sets #2 and #3) were evaluated. T-tests comparing rAd and Poly I:C responses to PBS in dLN were performed for this subset of modules. Poly I:C was found to regulate these modules in a manner highly comparable to the rAd vectors. At 8 hours, Poly I:C significantly (FDR < 0.01) regulated 16 modules (compared to 4-16 modules for the rAds) and the directionality of regulation by Poly I:C was

equivalent to the directionality of regulation by the rAd vectors for the 17 modules with consistent directionality for all 7 vectors. At 24 hours, Poly I:C significantly regulated 12 modules (compared to 7-16 modules for the rAd vectors) and the directionality of regulation by Poly I:C was equivalent to the directionality of regulation by the rAd vectors for the 16 modules with consistent directionality for all 7 vectors. At 72 hours, Poly I:C significantly regulated 11 modules (compared to 0-11 modules for the rAd vectors) and the directionality of regulation by Poly I:C was equivalent to the directionality of regulation by the rAd vectors for 16/18 of the modules with consistent directionality for all 7 vectors. These results demonstrate that Poly I:C very comparably activates the innate immunity pathways triggered by rAd vectors. Similar results were obtained when the analysis was applied to the 3888 genes regulated by the rAd vectors (Figure 4A, Supplemental Table 1).

10.2 - Exhaustive analysis: A similar strategy to step 3 (above) was taken to exhaustively identify genes with innate immune responses to Poly I:C that differed from responses consistently induced by rAd vectors. The preliminary process from step 3 was essentially unchanged except that the levels of the fixed Vector effect (V) were expanded to include Poly I:C (n = 4 replicates at 8, 24 and 72 hours). An additional step was included in which pair-wise T-tests were employed to compare responses to Poly I:C to each rAd vector response at each time point. Requirements for subsequent gene selection included: (i) at a given time point, significant (FDR < 0.05) differences were observed between Poly I:C and all rAd vectors; (ii) the directionality of the differences with Poly I:C was consistent for all rAd vectors; and (iii) at least 2-fold average expression difference was observed between Poly I:C and

all rAd vectors. In this manner, 38, 57 and 86 genes were identified at 8, 24 and 72 hours post-vaccination that exhibit Poly I:C-induced innate immune responses that differ significantly to the rAd vectors (data not shown). These results demonstrate that, despite gross similarity, some innate immune responses triggered by rAd vectors and Poly I:C are distinct. Further work is necessary to determine the functional importance of these responses in programming adaptive immunity.

Step 11 - Comparing responses to chAd63 in WT and IFNαβR -/- mice

Two analyses were performed that compared the innate transcriptional responses triggered by chAd63 in WT and IFNαβR -/- mice at the 8 hour time point.

10.1 - Candidate analysis: In the candidate-based analysis of the difference between innate immune responses induced by chAd63 in WT and IFNαβR -/- mice, the 23 modules significantly regulated by all vectors in dLN (co-expression modules C1-14 and the nine significantly regulated modules from Module Sets #2 and #3) were evaluated. T-tests comparing responses induced by chAd63 with PBS controls were performed for this subset of modules in dLN from WT and IFNαβR -/- mice. For reference, responses induced by rAd5 in this same set of experiments were also analysed. Although chAd63 was found to significantly (FDR < 0.001) regulate 15 modules in WT mice, no modules were significantly impacted by chAd63 in IFNαβR -/- mice. Four modules were significantly affected by rAd5 in the WT mice in these experiments. If the threshold for statistical significance is relaxed to FDR < 0.3, the number of significantly regulated modules increased to 21, 13 and 2 for chAd63 in WT mice, rAd5 in WT mice and chAd63 in IFNαβR -/- mice, respectively. The two

modules regulated by chAd63 in dLN from IFNαβR -/- mice are co-expression modules C2 (IFN signaling) and C3 (IFNs). These results indicate that type I IFN signaling deficiency appreciably dampens chAd63-induced innate immune responses, but they are not completely ablated. Similar results were obtained from analyses at the gene level.

11.2 - Exhaustive analysis: Given that the two IFN-associated co-expression modules exhibited marginal residual expression in IFNαβR -/- mice, an exhaustive analysis was carried out to identify the complete set of genes giving rise to these responses. This analysis proceeded similarly to step 3 (above). Starting from 35540 unique genes, 14117 genes exhibiting 90% normalised log2 expression intensity quantiles that exceeded a value of 8 were retained for subsequent analysis. Log2 expression values for each gene were standardised to fold changes with respect to PBS by subtracting the overall average log2 PBS expression value (across all time points) for that gene in the same batch and/or mouse strain. Genes with log2 expression values that were significantly affected by vaccination (different between vectors and/or PBS) were then identified using F-tests (ANOVA in R) to compare two different linear expression models:

Model6: l2e ~ V + G + V:G

Model7: l2e ~ G

In these models, "l2e" is the batch/tissue standardised log2 expression fold change for the gene compared to PBS, V is the fixed effect for vector (levels: PBS, chAd63), G

is the fixed effect for genotype (levels: WT, IFNαβR -/-) and V:G represents the vector*genotype interaction. P-values from the F-test comparing *Model6* and *Model7* were adjusted to FDRs using the Benjamini-Hochberg algorithm. The FDR threshold for significant impact of vaccination on expression was set at 0.001, which yielded 2889 genes. The subset of these genes robustly regulated in response to chAd63 vaccination in WT mice was then identified by comparing expression levels for PBS and chAd63 groups using a T-test, keeping only those genes with FDR < 0.001 and absolute average log2 fold change > 1. This yielded 1474 genes. The expression levels of these genes in the PBS and chAd63 groups in IFNαβR -/- mice were then compared by T-test. Although there were no genes reaching a stringent threshold for differences (FDR < 0.001), relaxing the FDR cutoff to 0.3 and requiring absolute average log2 fold change > 0.5 yielded 22 genes exhibiting robust responses in dLN from *IFNαβ*R -/-mice (Figure 12I). These genes include chemokines (Ccl2, Ccl7, Cxcl1, Cxcl10), cytokines (Ifna12, Ifna2, Ifnb1, Il1b) and IFN response genes (Ifit1, Isg15, and Rsad2).

Step 12 - Comparing responses to chAd63 in WT and STING gt/gt mice

Two candidate analyses were performed to assess the difference in innate immune responses induced by chAd63 in WT and *STING* gt/gt mice. In the first, the 23 modules significantly regulated by all vectors in dLN (co-expression modules C1-14 and the nine significantly regulated modules from Module Sets #2 and #3) were evaluated. T-tests comparing responses induced by chAd63 with PBS controls were performed for this subset of modules in dLN from WT and *STING* gt/gt mice. For

reference, responses induced by rAd5 in this same set of experiments were also analysed. As described above, chAd63 was found to significantly (FDR < 0.001) regulate 15 modules in WT mice, while (similarly to *IFNαβR* -/- mice) no modules were significantly impacted by chAd63 in *STING* gt/gt mice. Four modules were significantly affected by rAd5 in the WT mice in these experiments. If the threshold for statistical significance is relaxed to FDR < 0.3, the number of significantly regulated modules increases to 21, 13 and 14 for chAd63 in WT mice, rAd5 in WT mice and chAd63 in *STING* gt/gt mice, respectively. The fourteen modules regulated by chAd63 in dLN from *STING* gt/gt mice at this more permissive threshold include C3 (IFNs), but not C2 (IFN signaling), indicating that the residual responses to chAd63 in *STING* gt/gt mice overlap partially, but not completely, with those observed in *IFNαβR* -/- mice.

In the second candidate analysis, the expression of the 22 genes exhibiting residual induction in response to chAd63 in *IFNαβR* -/- mice was evaluated in *STING* gt/gt mice (Figure 12I). Only two of the 22 genes (Ccl2 and Ccl7) exhibited residual induction in response to chAd63 in *STING* gt/gt mice (FDR <0.3, avg log2 FC > 0.5), and these responses were strongly attenuated compared to those observed in *IFNαβR* -/- mice (Figure 12I).

Supplemental References:

1. Gentleman RC, et al. Bioconductor: open software development for computational biology and bioinformatics. *Gen Biol*. 2004;5(10):R80.
2. Eisen MB, Spellman PT, Brown PO, Botstein D. Cluster analysis and display of genome-wide expression patterns. *Proc Natl Acad Sci USA*. 1998;95(25):14863-14868.
3. Zuberi K, et al. GeneMANIA prediction server 2013 update. *Nuc Acids Res*. 2013;41(Web Server issue):W115-122.
4. Chaussabel D, et al. A modular analysis framework for blood genomics studies: application to systemic lupus erythematosus. *Immunity*. 2008;29(1):150-164.
5. Obermoser G, et al. Systems scale interactive exploration reveals quantitative and qualitative differences in response to influenza and pneumococcal vaccines. *Immunity*. 2013;38(4):831-844.
6. Jojic V, et al. Identification of transcriptional regulators in the mouse immune system. *Nat Immunol*. 2013;14(6):633-643.
7. Zak DE, et al. Merck Ad5/HIV induces broad innate immune activation that predicts CD8+ T-cell responses but is attenuated by preexisting Ad5 immunity. *Proc Natl Acad Sci USA*. 2012;109(50):E3503-12.
8. Coordinators NR. Database resources of the National Center for Biotechnology Information. *Nuc Acids Res*. 2014;42(Database issue):D7-17.
9. Li S, et al. Molecular signatures of antibody responses derived from a systems biology study of five human vaccines. *Nat Immunol*. 2014;15(2):195-204.

10. de Leeuw WC, Rauwerda H, Jonker MJ, Breit TM. Salvaging Affymetrix probes after probe-level re-annotation. *BMC Res Notes*. 2008;1:66.

11. Querec TD, et al. Systems biology approach predicts immunogenicity of the yellow fever vaccine in humans. *Nat Immunol*. 2009;10(1):116-125.

<u>Supplemental Figure 1:</u> Hierarchy of CD8 T cell response magnitude after rAd vaccination in blood or tissue

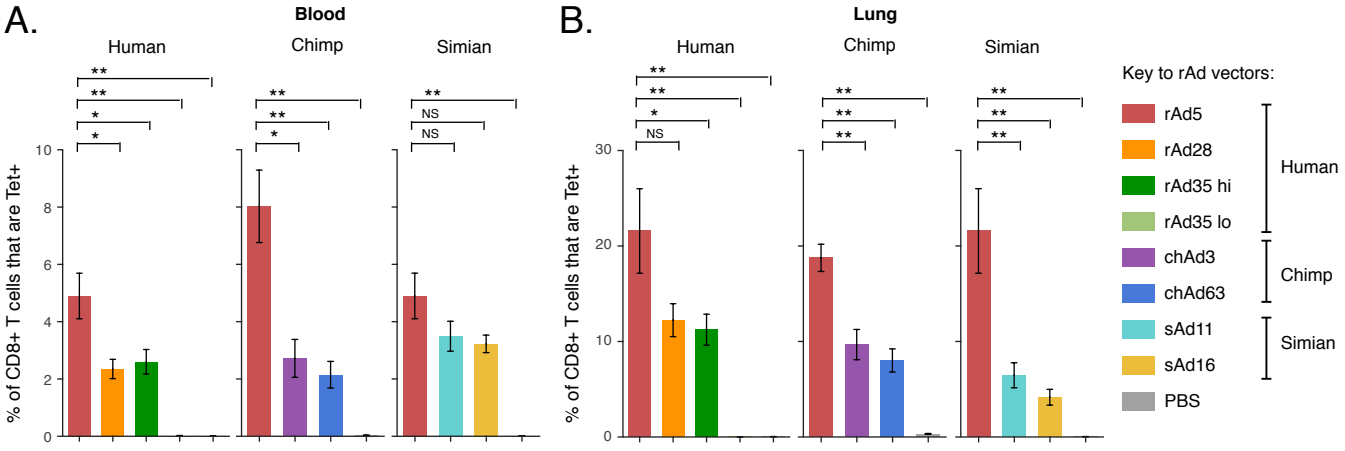

<u>Supplemental Figure 2:</u> Gating strategy for defining DC subsets in vivo

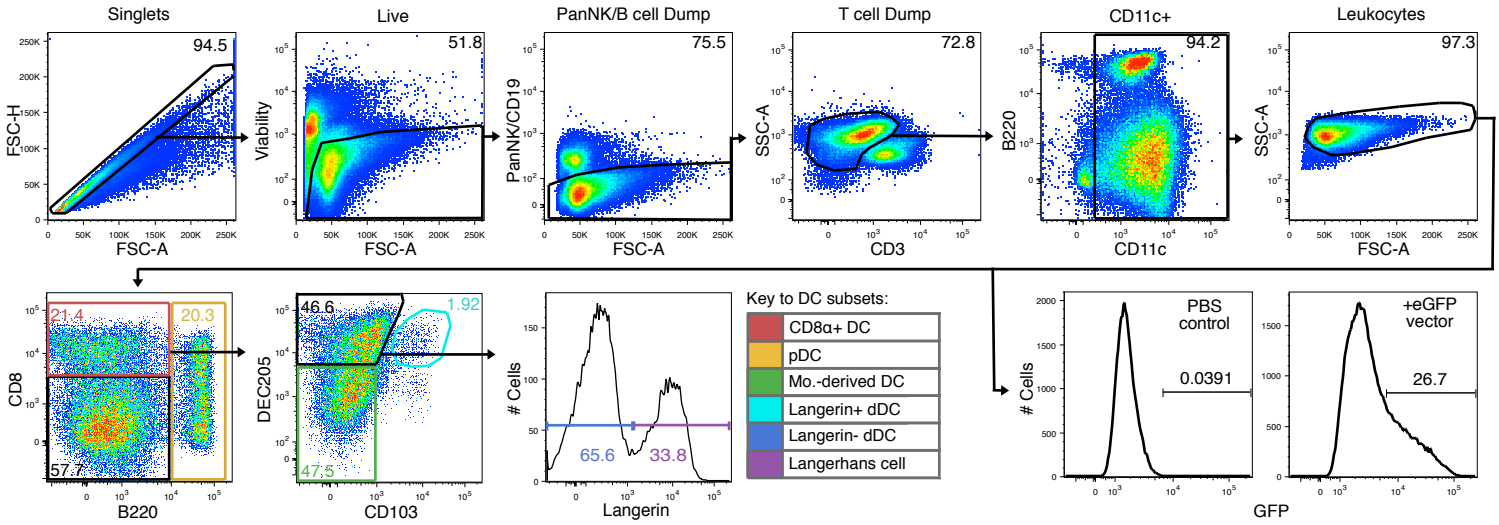

Supplemental Figure 3: Distribution of Ag to DC subsets after rAd vaccination at varying doses.

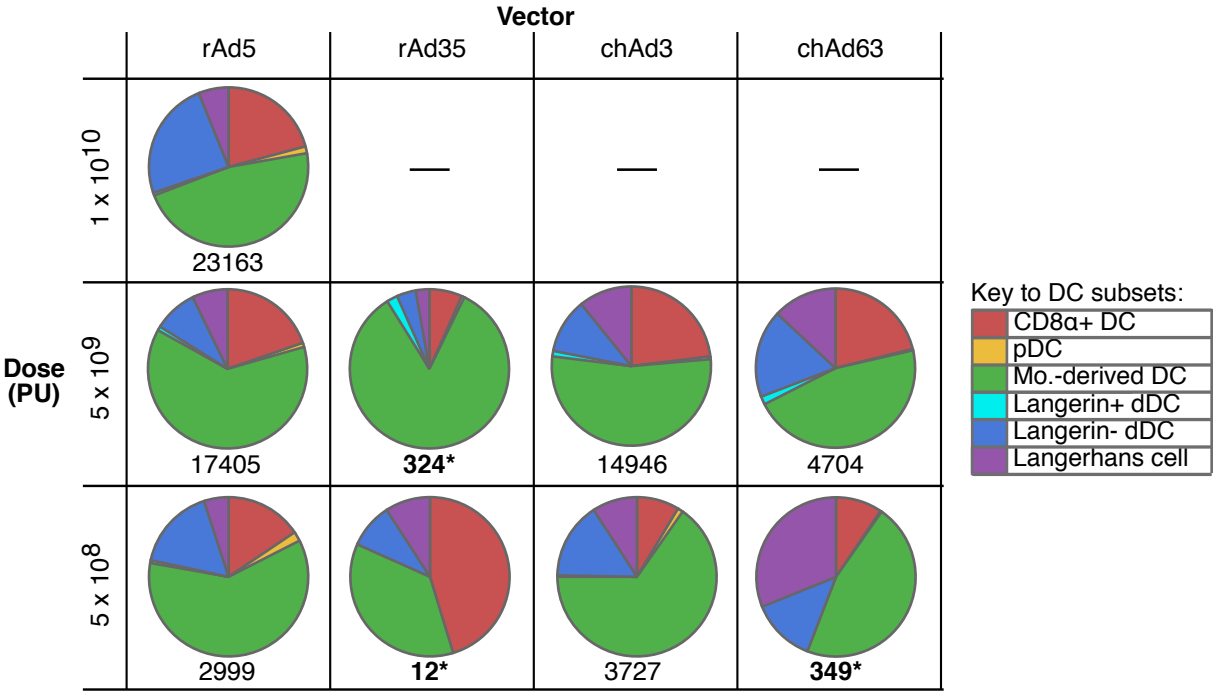

<u>Supplemental Figure 4:</u> Role of NK cells in the CD8 T cell response to rAd vaccination

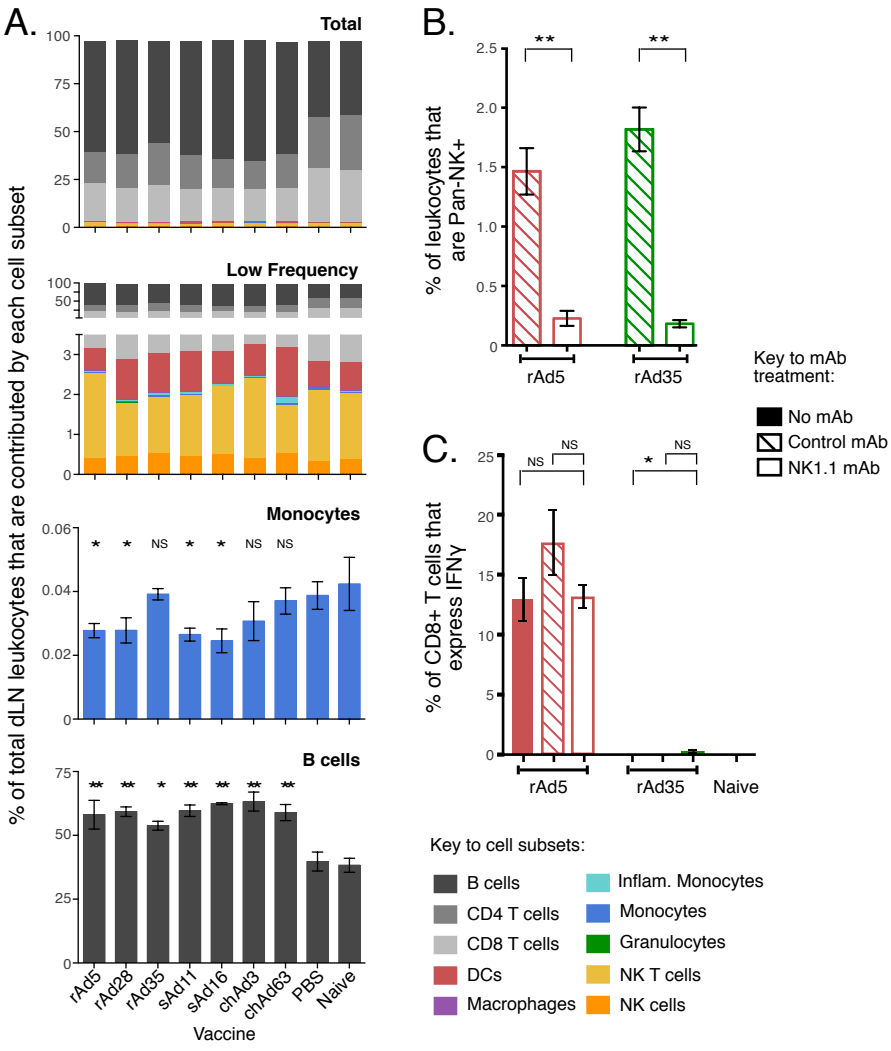

Supplemental Figure 5: Type I IFN and IP-10 production after rAd vaccination in STING gt/gt mice

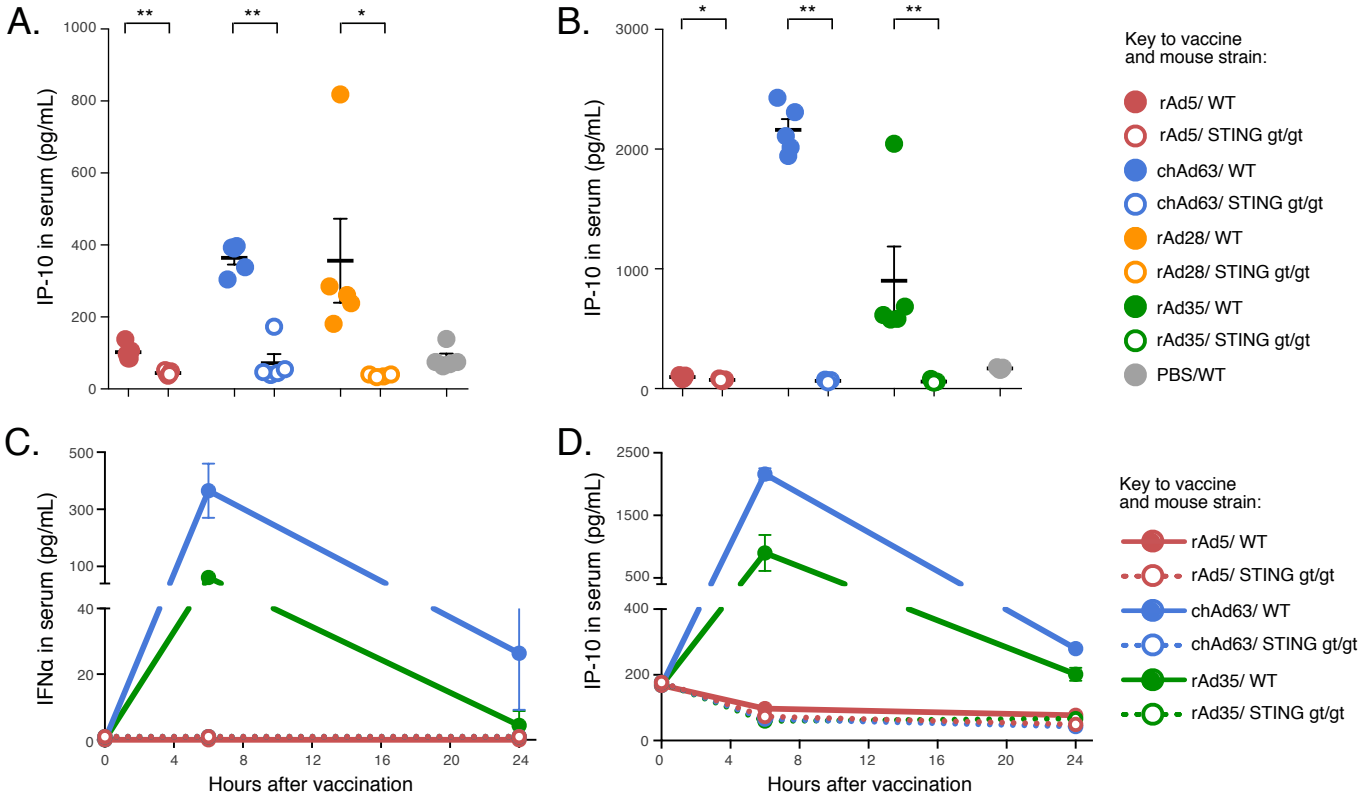

Supplemental Figure 6: CD8 T cell responses after rAd28 vaccination in STING gt/gt mice

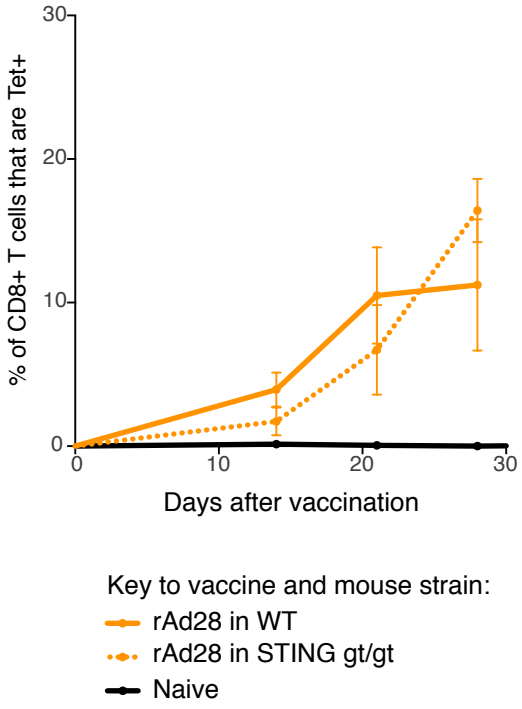

Supplemental Figure 7: CD8 T cell memory and secondary responses after rAd vaccination in STING gt/gt mice.